

Research Article

Mechanical Behavior of Frozen Porous Sandstone under Uniaxial Compression

Hong-Ying Wang¹ and Qiang Zhang²

¹School of Transportation Engineering, Jiangsu Vocational Institute of Architectural Technology, Xuzhou 221116, China

²State Key Laboratory for Geomechanics and Deep Underground Engineering, China University of Mining & Technology, Xuzhou 221116, China

Correspondence should be addressed to Qiang Zhang; qzhang@cumt.edu.cn

Received 28 June 2021; Accepted 23 August 2021; Published 14 September 2021

Academic Editor: Zetian Zhang

Copyright © 2021 Hong-Ying Wang and Qiang Zhang. This is an open access article distributed under the Creative Commons Attribution License, which permits unrestricted use, distribution, and reproduction in any medium, provided the original work is properly cited.

The influence of low temperature on longitudinal wave velocity, uniaxial compression strength, tensile strength, peak strain, secant modulus, and acoustic emission characteristics of yellow sandstones was studied. The results show that the secant modulus increases with decreasing temperature when the axial strain is less than 0.6%, and a contrary influence performs for the subsequent stage due to the fracture of the pore ice. With the decrease in temperature, the uniaxial compression strength first increases and then remains at a relatively constant value of 34.44 MPa at about -40°C while the temperature ranges from -40°C to -70°C . The tensile strength shows an approximate linear increment as the temperature. The peak strain gradually increases with temperature in a three-stage piecewise linear form, and the increasing rate gradually decreases with the decreasing temperature. The phase transformation from liquid water at a temperature of 20°C to solid ice at a temperature of -3°C significantly increases the longitudinal wave velocity from 1.55 km/s to 3.36 km/s. When the temperature is lower than -10°C , the longitudinal wave velocity approximately increases linearly at a rate of $2.67 \times 10^{-3} \text{ km/s} \cdot ^{\circ}\text{C}^{-1}$ with decreasing temperature.

1. Introduction

The mechanical properties of porous rock mass in a water-rich stratum at subzero temperature are of significance for the construction of highways, artificial freezing in a vertical shaft and metro, and storage and mining in cold regions such as the Tibet Plateau and Xinjiang district [1]. Subzero temperature can induce thermal effects, i.e., phase transition of water and frost heave, which results in significant changes in the mechanical properties of rocks [2]. The mechanical properties are a basic consideration for the design and stability evaluation of engineering. Therefore, the influence of temperature on the mechanical properties of rocks should be thoroughly investigated.

Many achievements have been obtained in the past decades. The experimental results denote that the strength, elastic modulus [3, 4], fracture toughness [5], and accumula-

tive acoustic emission (AE) quantities [6] increase with decreasing temperature. The effects of cyclic loading-unloading [7], explosion [8], and chemical corrosion [9] decrease the strength, elastic modulus, and Poisson's ratio of rock samples. Additionally, the strength and modulus gradually decrease with the increase in frost-thaw cycle times [10–14]. A series of constitutive models have been proposed for frozen sandstone considering the loading ratio effect [7]. Among these studies, the frozen temperature is within $-20\sim 20^{\circ}\text{C}$ according to the standard requirements of the International Society of Rock Mechanics (ISRM), and the red sandstone is widely used with a porosity less than 10% [15]. However, in particle engineering, the environment temperature is much lower than -20°C , and the porosity of rock samples is much larger than 10% [4].

Due to the much lower temperature and higher porosity, the rocks may perform different mechanical behaviors from

the conventional results, which has not been investigated. In this study, the experiments on frozen saturated yellow sandstones with a porosity of 13.08% at a wide range of temperature $-70\sim-20^{\circ}\text{C}$ are conducted to investigate the mechanical behaviors, including compression strength, tensile strength, deformation characteristics, and AE characteristics according to the uniaxial compression test. This study can provide some references for the construction and development of structures in high porosity rocks in very cold regions.

2. Experimental Details

The yellow sandstone blocks with a porosity of 13.08% and a dry density of 2.10 g/cm^3 were retrieved from Daban district, Xinjiang, China, where the minimum temperature reaches -41°C . According to the requirements of ISRM, the parallelism was controlled within $\pm 0.05\text{ mm}$ and the surface flatness within $\pm 0.02\text{ mm}$. Standard cylindrical specimens with a diameter of 50 mm and heights of 100 mm and 25 mm for compression and Brazilian Split tests were prepared. And samples with similar initial longitudinal wave velocity tested using RSM-SY6 were selected. Three rock samples were carried out for the same experimental condition to avoid the random error induced by the discreteness of rock.

The uniaxial compression tests were conducted with the electrohydraulic servocontrolled material testing machine MTS810, and the saturated samples were frozen using the low-temperature furnace MTS615.06 with a rate of $-1.0^{\circ}\text{C}/\text{min}$. Eight temperature levels of 20, -3, -10, -20, -40, -50, -60, and -70°C were selected. When the environment temperature reached the preset value, the temperature was maintained for 30 mins. Then, the uniaxial compression tests were carried out with a loading rate of 0.002 mm/s . During the compression test process, the AE signal was detected and recorded using a DS5-8A.

3. Results and Analysis

3.1. Stress-Strain Behavior. Figure 1 shows the strain-stress curves at various temperatures. The elastic behavior is divided into two stages, i.e., hardening stage and weakening stage, by the inflection point of $\epsilon_1 = 0.6\%$. For the specimens at a relatively high temperature (i.e., $T > -10^{\circ}\text{C}$), an obvious compaction behavior is observed in the hardening stage. With the decrease in temperature, the compaction behavior becomes unsuspecting instead of an initial approximately linear behavior. For the specimens with $T < -20^{\circ}\text{C}$, the initial elastic modulus increases more significantly than that for $T > -20^{\circ}\text{C}$. When the temperature is lower than -30°C , the strain-stress curve turns from a concave shape to a convex curve. Contrary to the hardening stage, the secant modulus at the weakening stage decreases with the decreasing temperature. A brittle failure occurs with a sudden drop in strength when the peak strength is reached. The vibration in stress-strain behavior due to freezing temperature is mainly induced by the pore frozen ice, which fractures at an axial strain of 0.6% [16].

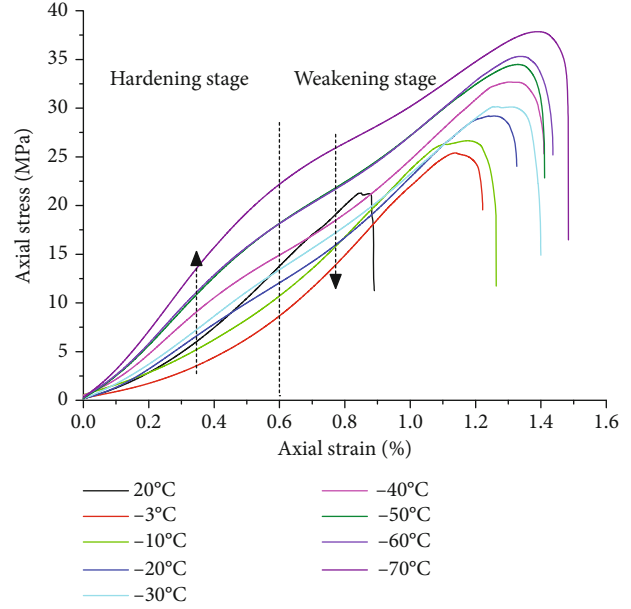


FIGURE 1: Uniaxial compressive stress-strain curves at various temperatures.

At the initial frozen stage within $-3\sim-10^{\circ}\text{C}$, the volume and strength of ice significantly increases. Due to the filling of porous ice, the relative movement of the matrix is constrained, which enhances the whole stiffness and reduces the concentration effect. Thus, with the same axial strain, the potential sample cracks at a lower temperature are less than those at a higher temperature, which leads to the initial enhanced stress-strain behavior, i.e., the hardening stage. Once the strain reaches the critical strain of ice, fracture simultaneously occurs. Due to the enhanced strength for lower temperature frozen rock, the friction coefficient of the fracture surface would be much smaller than that of samples at a higher temperature. Thus, in the weakening stage, the stiffness of the sample at a lower temperature is less than that at a higher temperature.

3.2. Variations in Uniaxial Compression Strength and Tensile Strength. Figure 2 shows the evolutions of uniaxial compressive strength (UCS) and tensile strength with temperature. The UCS gradually increases with the decreasing temperature in a piecewise linear manner as shown in Figure 2(a). When the temperature decreases from 20 to -3°C , the UCS increases from an average value of 20.41 MPa to 23.69 MPa at an increase rate of 16.07%. Then, the UCS increases to 34.01 MPa at an increase rate of 43.56% for specimens subjected to temperatures within $-3\sim-40^{\circ}\text{C}$, and the strength increases at an average rate of $-0.28\text{ MPa}/^{\circ}\text{C}$ with temperature. This is the same as the strength evolution of ice, which sharply increases within $0\sim-10^{\circ}\text{C}$, then remains as a linear increase at a smaller rate [17]. In fact, the increase in strength is mainly induced by the increasing ice strength. However, a larger volume expansion also induces internal force and potential cracks, if any. Thus, when the temperature is lower than -40°C , potential cracks may form inside the sandstone, which will induce the whole strength. Under

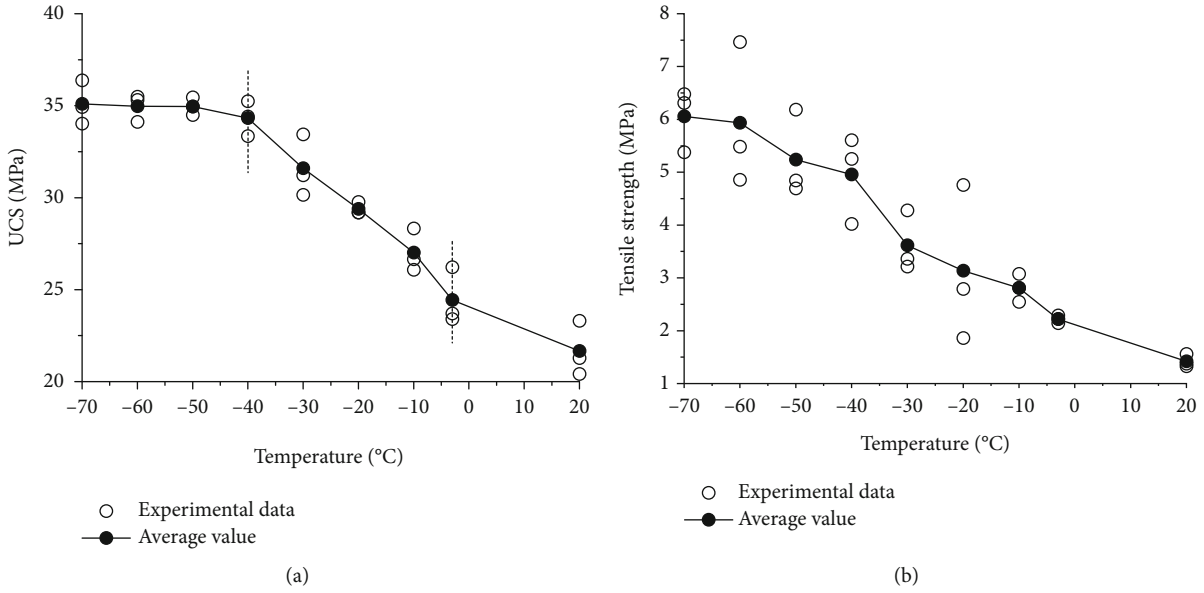


FIGURE 2: Evolutions of UCS and tensile strength with temperature: (a) UCS and (b) tensile strength.

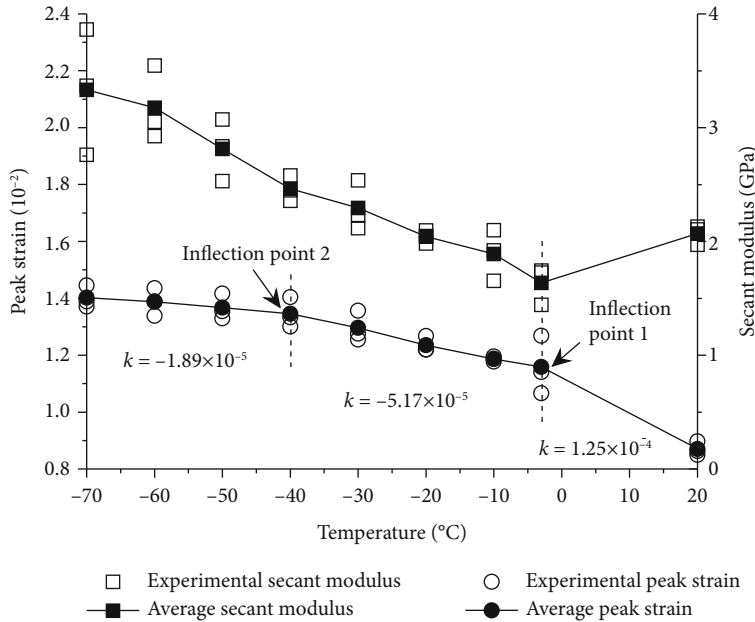


FIGURE 3: Evolution of peak strain and secant modulus with temperature.

the above two influences, a slight increase in UCS occurs with an average increase of 0.78 MPa for the specimen at -40°C and -70°C, and the mean UCS of specimens within -40~-70°C is 34.44 MPa. Thus, -40°C is the critical temperature, which distinguishes the influence of temperature on the strength of porosity yellow sandstone.

The tensile strength based on the Brazilian test is calculated by the formula as follows:

$$\sigma_t = \frac{2P}{\pi Dt}, \quad (1)$$

where σ_t is the tensile strength, P is the peak load, D is the diameter of the disc, and t is the thickness of the disc.

The tensile strength of yellow sandstone samples changes significantly along with the temperature as shown in Figure 2(b). The tensile strength is 1.42 MPa, 2.22 MPa, 4.96 MPa, and 6.06 MPa corresponding to a temperature of 20°C, -3°C, -40°C, and -70°C, respectively, showing an approximate linear increase with the decreasing temperature. For the frozen samples, the average increasing rate of the tensile strength with temperature is 0.07 MPa/°C. However, when the temperature is lower than -40°C, the increasing rate in the tensile strength decreases. The average

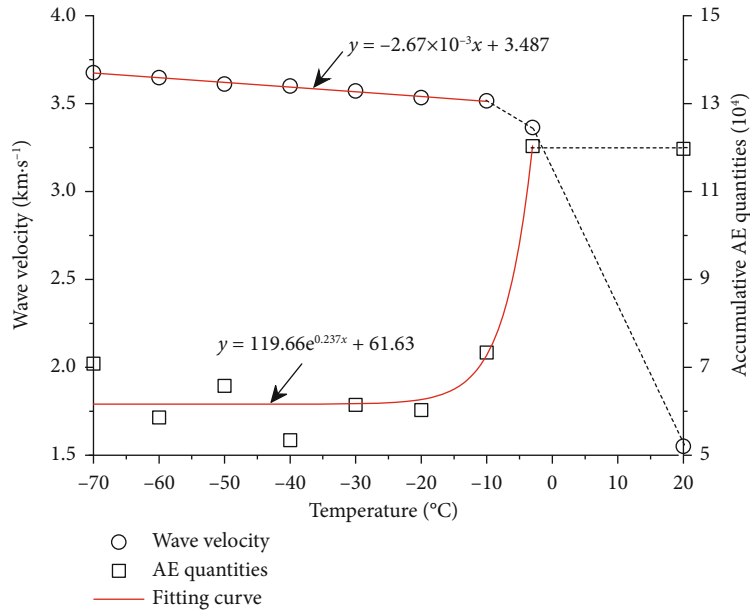


FIGURE 4: Influence of temperature on longitudinal wave velocity and AE characteristics.

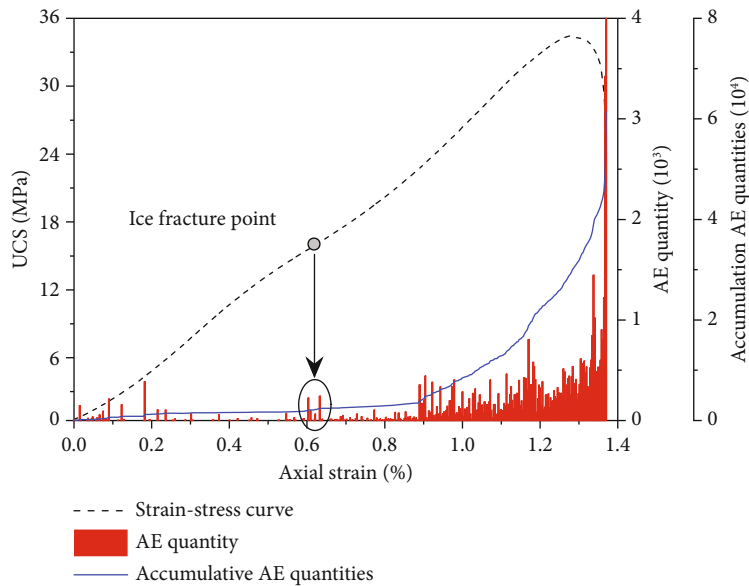


FIGURE 5: Acoustic emission characteristics of specimen at $T = -30^{\circ}\text{C}$.

increasing rate in the tensile strength is only $0.03 \text{ MPa}/^{\circ}\text{C}$ for samples within $-40^{\circ}\text{C}\sim-70^{\circ}\text{C}$.

3.3. Variations in Peak Strain and Secant Modulus. Figure 3 shows the evolutions of peak strain and secant modulus with temperature. Similar to the evolution of UCS, the peak strain (strain corresponds to the peak strength) gradually increases in a three-stage linear manner as temperature decreases by two inflection temperatures of -3°C and -40°C . When the temperature decreases from 20°C to -3°C , the peak strain increases from an average value of 0.87% to 1.16% with a rate of $-1.25 \times 10^{-4} \text{ }^{\circ}\text{C}^{-1}$ with decreasing temperature. For temperatures within $-10\sim-40^{\circ}\text{C}$ and $-40\sim-70^{\circ}\text{C}$, the peak strain decreases to 1.35% and 1.40% with the rates of

$-5.17 \times 10^{-4} \text{ }^{\circ}\text{C}^{-1}$ and $-1.89 \times 10^{-4} \text{ }^{\circ}\text{C}^{-1}$, respectively. This is influenced by pore ice, which constrains the deformation of the rock matrix. A lower temperature corresponds to a larger stiffness of ice and a more significant constriction effect.

The secant modulus performs a two-piecewise characteristic with temperature. When the temperature decreases from 20°C to -3°C , the secant modulus decreases from 2.07 GPa to 1.64 GPa , at a decrease rate of 20.77% . This is mainly induced by the expansion damage during the phase transition of water. However, for the frozen samples, the secant modulus shows an approximate linear increase as the decreasing temperature. When the temperature decreases to -20°C , the secant modulus increases to

2.04 GPa, which approximately equals to that at $T = 20^{\circ}\text{C}$. Compared to the secant modulus at $T = -3^{\circ}\text{C}$, the secant modulus increases to an average value of 3.33 GPa for the specimen at $T = -70^{\circ}\text{C}$, at an increase rate of 103.05% with respect to that at $T = -3^{\circ}\text{C}$. The average increasing rate in the secant modulus is $0.025 \text{ MPa}/^{\circ}\text{C}$ for subzero temperature specimens.

3.4. Variations in Peak Strain and Secant Modulus. Figure 4 shows the influence of temperature on the longitudinal wave velocity and accumulative AE characteristics. The transformation from liquid water at a temperature of 20°C to solid ice at a temperature of -3°C in the pore of yellow sandstone increases the longitudinal wave velocity from 1.55 km/s to 3.36 km/s. When the temperature further decreases to -10°C , the velocity increases to 3.52 km/s [18] and keeps an average increasing rate of $-2.67 \times 10^{-3} \text{ km/s} \cdot ^{\circ}\text{C}^{-1}$ for the temperatures from -10 to -70°C . Thus, the initial solid stage of water significantly increases the longitudinal wave velocity. With the decrease in temperature when $T < -10^{\circ}\text{C}$, the increase in amplitude gradually decreases and remains at approximately a constant value.

During the initial freezing process, the accumulative AE qualities change a little, which increases from $11.97e4$ to $12.03e4$. With a further decreasing temperature from -3°C to -70°C , the accumulative AE quantities follow an exponentially decreasing manner with a decreasing decay rate. For specimens at $T = -30^{\circ}\text{C}$, the accumulative AE quantities are $6.15e4$ at a decrease rate of 48.76% corresponding to that at $T = -3^{\circ}\text{C}$. Figure 5 shows the typical AE characteristics at $T = -30^{\circ}\text{C}$. Obviously, a series of significant AE rings occur at an axial strain of 0.6% corresponding to the ice fracture strain. Before this point, there is a silence period, in which only a few AE rings occur due to the compaction of initial cracks. The AE characteristics subsequently become active, and the AE ring quantity increases robustly after the fracture of ice.

4. Conclusions

A series of uniaxial compression tests and Brazilian tests were carried out at a wide range of temperature within -70 – 20°C . The results show that the stress-strain curves are divided into two stages by the axial strain of 0.6%, which corresponds to the approximate fracture point of ice. In the initial stage, the second modulus gradually enhances with the decreasing temperature; however, a decreasing modulus performs in the second stage. The uniaxial compressive strength firstly shows a linear increase for temperatures within -3 – -40°C at an average rate of $-0.28 \text{ MPa}/^{\circ}\text{C}$. Then, the uniaxial compressive strength remains approximately constant value of 34.44 MPa subjected to temperatures within -40 – -70°C . With the decreasing temperature, an approximate linear increase in tensile strength is performed. With the decrease in temperature, the peak strain shows a three-stage piecewise increasing characteristic, and the increasing rates of $-1.25 \times 10^{-4} \text{ }^{\circ}\text{C}^{-1}$, $-5.17 \times 10^{-5} \text{ }^{\circ}\text{C}^{-1}$, and $-1.89 \times 10^{-4} \text{ }^{\circ}\text{C}^{-1}$ correspond to the temperature ranges of -3 – 20°C , -20 – -40°C , and -70 – -40°C , respectively. The

phase change from liquid water to solid ice significantly increases the longitudinal wave velocity, and an increasing rate of $-2.67 \times 10^{-3} \text{ km/s} \cdot ^{\circ}\text{C}^{-1}$ remains for specimens at a temperature that is lower than -10°C . The freezing water changes a little in accumulative acoustic emission quantities, and a further exponential decrease occurs for subzero samples.

Data Availability

Anyone who needs the data in the manuscript can contact the corresponding author with email address of qzhang@cumt.edu.cn.

Conflicts of Interest

The authors declare that they have no conflicts of interest.

Acknowledgments

The authors are grateful for the financial support from the National Natural Science Foundation of China (52074269) and China Postdoctoral Science Foundation (2020T130698).

References

- [1] A. Kenji and H. Keisuke, "Storage of refrigerated liquefied gases in rock caverns: characteristics of rock under very low temperatures," *Tunnelling and Underground Space Technology*, vol. 5, no. 4, pp. 319–325, 1990.
- [2] Y. Inada and K. Yokota, "Some studies of low temperature rock strength," *International Journal of Rock Mechanics and Mining Sciences & Geomechanics Abstracts*, vol. 21, no. 3, pp. 145–153, 1984.
- [3] C. Park, J. Synn, H. Shin, D. Cheon, H. Lim, and S. Jeon, "An experimental study on the thermal characteristics of rock at low temperatures," *International Journal of Rock Mechanics and Mining Sciences*, vol. 41, no. 3, pp. 367–368, 2004.
- [4] T. Yamabe and K. M. Neaupane, "Determination of some thermo-mechanical properties of Sirahama sandstone under subzero temperature condition," *International Journal of Rock Mechanics and Mining Sciences*, vol. 38, no. 7, pp. 1029–1034, 2001.
- [5] N. Matsuoka, "Mechanisms of rock breakdown by frost action: an experimental approach," *Cold Regions Science and Technology*, vol. 17, no. 3, pp. 253–270, 1990.
- [6] B. Liu, G. Zhang, W. Xu, and L. Liu, "Acoustic emission characterization of frozen sandstone in uniaxial compression test," in *50th US Rock Mechanics/Geomechanics Symposium*, Houston, Texas, 2016.
- [7] N. Li, P. Zhang, W. Chen, and G. Swoboda, "Fatigue properties of cracked, saturated and frozen sandstone samples under cyclic loading," *International Journal of Rock Mechanics and Mining Sciences*, vol. 40, no. 1, pp. 145–150, 2003.
- [8] J. Bonner, M. Leidig, C. Sammis, and R. Martin, "Explosion coupling in frozen and unfrozen rock: experimental data collection and analysis," *Bulletin of the Seismological Society of America*, vol. 99, no. 2A, pp. 830–851, 2009.
- [9] X. Fang, J. Xu, and P. Wang, "Compressive failure characteristics of yellow sandstone subjected to the coupling effects of

- chemical corrosion and repeated freezing and thawing,” *Engineering Geology*, vol. 233, pp. 160–171, 2018.
- [10] T. Chen, M. Yeung, and N. Mori, “Effect of water saturation on deterioration of welded tuff due to freeze-thaw action,” *Cold Regions Science and Technology*, vol. 38, no. 2-3, pp. 127–136, 2004.
- [11] W. Chen, X. Tan, H. H. Yu, K. Yuan, and S. Li, “Advance and review on thermo-hydro-mechanical characteristics of rock mass under condition of low temperature and freeze-thaw cycles,” *Chinese Journal of Rock Mechanics and Engineering*, vol. 30, no. 7, pp. 1318–1336, 2011.
- [12] M. Zhou and G. Meschke, “A multiscale homogenization model for strength predictions of fully and partially frozen soils,” *Acta Geotechnica*, vol. 13, no. 1, pp. 175–193, 2018.
- [13] M. Zhou and G. Meschke, “Strength homogenization of matrix-inclusion composites using the linear comparison composite approach,” *International Journal of Solids and Structures*, vol. 51, no. 1, pp. 259–273, 2014.
- [14] E. Liu, Y. Lai, M. Liao, X. Liu, and F. Hou, “Fatigue and damage properties of frozen silty sand samples subjected to cyclic triaxial loading,” *Canadian Geotechnical Journal*, vol. 53, no. 12, pp. 1939–1951, 2016.
- [15] M. Tang, Z. Wang, Y. Sun, and J. Ba, “Experimental study of mechanical properties of granite under low temperatures,” *Chinese Journal of Rock Mechanics and Engineering*, vol. 29, no. 4, pp. 787–794, 2010.
- [16] M. Zhang, *Experimental Study on Uniaxial Compressive Strength of Ice and Influence Factors*, Dalian University of Technology, 2012.
- [17] D. M. Anderson and W. F. Weeks, “A theoretical analysis of sea-ice strength,” *Transactions, American Geophysical Union*, vol. 39, no. 4, pp. 632–640, 1958.
- [18] D. Draebing and M. Krautblatter, “P-wave velocity changes in freezing hard low-porosity rocks: a laboratory-based time-average model,” *Cryosphere Discussions*, vol. 6, no. 5, pp. 1163–1174, 2012.